CMLS, Cell. Mol. Life Sci. 61 (2004) 1354–1365
1420-682X/04/111354-12
DOI 10.1007/s00018-004-4010-6

CMLS Cellular and Molecular Life Sciences

Research Article

Occludin binds to the SH3-hinge-GuK unit of zonula occludens protein 1: potential mechanism of tight junction regulation

A. Schmidt [a], D. I. Utepbergenov [a], S. L. Mueller [a], M. Beyermann [a], J. Schneider-Mergener [b] G. Krause [a] and I. E. Blasig [a,*]

[a] Forschungsinstitut für Molekulare Pharmakologie, Robert-Rössle-Str. 10, 13125 Berlin (Germany), Fax: +49 30 94793 243, e-mail: iblasig@fmp-berlin.de
[b] Institut für Medizinische Immunologie, Charite, Humboldt-Universität, Berlin (Germany)

Received 12 January 2004; received after revision 23 February 2004; accepted 31 March 2004

Abstract. The interaction between tight junction proteins occludin and zona occludens protein 1 (ZO-1) was clarified. The sequence cc1 within the hinge region of ZO-1, connecting its SH3 and GuK domains, was identified as a new association site for the occludin C-terminus, core binding area G**L**RSSKRN**L**RKSR (mouse ZO-1$^{606-618}$). Occludin also bound to the sequence H2 within GuK, core area HKLRKNNH (ZO-1$^{759-766}$). In occludin, the binding core was E**L**SRLDKE**L**DDYREESEEY (mouse occludin$^{455-473}$). Helicity of the sequences was suggested by circular dichroism. Because basic residues in ZO-1, acidic residues in occludin (underlined), coiled-coil helix-forming leucine heptad motifs (bold) in occludin and, probably, in cc1 were essential, we conclude that interactions were both helical and ionic. Moreover, the GuK domain bound other GuK molecules, suggesting oligomerization of ZO-1. Generally, the assumption is supported that the SH3-hinge-GuK region represents a functional and regulatory unit in ZO-1 forming a multiprotein tight junction complex with occludin.

Key words. ZO-1; occludin; tight junction; protein interaction; MAGuK protein family; adaptor protein.

Continuous tight junctions (TJs) seal endothelial and epithelial cell clefts in different organs and function as a diffusion barrier between adjacent cells [1, 2]. These barriers are relevant for organ function and can be modulated under physiological and pathological conditions [3]. An increasing number of proteins are being found in TJs [4], but the exact structure and function of the multiprotein complex is unclear. Defining how TJ proteins interact, therefore, is a prerequisite to understanding the barrier function at the molecular level.

Several scaffolding proteins are associated with TJs indicating a network of interacting proteins. The zona occludens proteins (ZO-1,-2,-3) belong to the membrane-associated guanylate kinase homologue protein (MAGuK) family. MAGuKs are composed of PDZ (PSD95/dlg/ZO-1), SH3 (src homology 3, consensus motive of SH3 domains), GuK (guanylate kinase homologue, sequence homologue to the GuK domain in guanylate kinase) domains, acidic and proline-rich regions [5]. They play a critical role in regulating protein assembly at cell-cell contacts [6], in tumor suppression [7], clustering of ion channels and receptors [8], differentiation [9], regulation of gene expression and binding to the cytoskeleton [10, 11]. Interactions between cytoplasmic and transmembrane proteins together with linkage to the cytoskeleton may recruit TJ proteins and may modulate the barrier function [12].

* Corresponding author.

ZO-1 may form a complex with ZO-2 or ZO-3 [13]. It interacts with TJ strand proteins of the claudin family through PDZ-1 [12, 14] and with junctional adhesion molecules via PDZ-3 [9]. ZO-1 may associate with the cytosolic C-terminal part of occludin [10, 15], but the mechanism and kinetics of the association, the structure of intracellular occludin parts, and the exact binding sequences of each protein are unknown. The interaction of ZO-1 with occludin and other proteins is assumed to play a significant role in the assembly of TJ structure and regulation of TJ function [16]. Occludin has four transmembrane domains with N- and C-terminal parts in the cytoplasm and two extracellular loops. Disruption of barrier properties is achieved through transfection of occludin mutants without extracellular [17] or intracellular [18] parts and by incubation with peptides from extracellular loops [19–21]. ZO-1 might, via its scaffolding function, organize occludin at TJs and regulate its function, since occludin remains diffusely stained at the cell surface of fibroblasts which do not express ZO-1 [20, 22].

In preliminary studies we have observed that the GuK domain of ZO-1 binds directly to occludin [23]. The X-ray structure from SH3 and GuK of synaptic MAGuK PSD-95 shows that both domains may form a common unit [24, 25]. From this, we hypothesize that a SH3-GuK unit is formed in ZO-1 also and that this unit, including a specific hinge region, associates with the cytosolic C-terminal end of occludin. The aim of the study, therefore, was to elucidate exact sequences and mechanisms responsible for the interaction between ZO-1 and occludin. In comparison with peptide epitope mapping, binding experiments were performed by surface plasmon resonance spectroscopy (SPR) adapted by us to study TJ proteins [23]. This is a new, direct, real-time, and quantitative approach to finding which segments of TJ proteins associate, and to what degree. The binding areas were narrowed down to core binding regions in both the hinge region and GuK domain of ZO-1, and in the last third of the occludin C-terminus. The data demonstrate that the interaction of ZO-1 and occludin is caused by differently charged helices, regulating the protein configuration at tight junctions.

Material and methods

Bioinformatic studies

To select amino acid sequences for binding studies, predictions of potential protein-protein interaction structures from ZO-1 and occludin were made by sequence analysis programs (fig. 1). Secondary-structure prediction algorithms used were Chou-Fassman, Garnier-Robson, and http://www.compbio.dundee.ac.uk/~www-jpred/ (DSC, PHD, PREDATOR, Zpred, Jnet). Predictions were accepted if at least six different subprograms came to the same result. The programs coilscan (GCG Program, GCG Wisconsin package; Accelrys Inc., San Diego, Calif.), and coils (http://www.ch.embnet.org/software/COILS_form.html), based on the algorithm of Lupas [27], were applied to predict potential coiled-coil helices.

Cloning of proteins and preparation of expression constructs

If not stated otherwise, mouse sequences were cloned via *Bam*HI and *Sal*I sites N-terminally fused with maltose binding protein (MBP; vector pMAL-c2X; NEB, Schwalbach, Germany) or glutathione-S-transferase (GST; vector pGEX-4T-1; Amersham Bioscience, Freiburg, Germany) in *Escherichia coli* (TOP10F′; Invitrogen, Breda, The Netherlands). cDNA encoding sequence ZO-1$^{601-890}$ (870 bp, including the GuK domain) was produced by RT-PCR from kidney [23]. Segments starting from ZO-1^{589} were derived using the corresponding primers. Sequences containing SH3 and GuK (ZO-1$^{502-812/502-803/502-794}$) were generated from human ZO-1 full-length cDNA in pCB6 (generous gift from A. Fanning, New Haven, Conn.). C-terminal cytosolic fragments of occludin were prepared from MBP-occludin$^{264-521}$ (777 bp) [23].

Overexpression and purification of proteins

The transformed cells were grown in rich medium (10 g/l tryptone, 5 g/l yeast extract, 125 mM NaCl, 10 mM glucose; Sigma-Aldrich, Steinheim, Germany) with 100 µg/ml ampicillin until absorbance (600 nm) of circa 0.6, and were induced by 0.3 mM isopropyl-β-D-thiogalactopyranoside (IPTG; Sigma-Aldich; 37 °C, 1.5 h). After centrifugation (2500 g, 7 min, 4 °C) and resuspension in 4 ml SP1 (20 mM Tris/HCl pH 7.8, 200 mM NaCl, 1 mM EDTA), cells were sonicated on ice 4 × 15 s. The lysate was centrifuged (20,000 × g, 4 °C, 2 min) and filtered (0.2 µm). MBP fusion proteins were bound to an amylose-resin column (NEB, Schwalbach, Germany), washed with SP1 and SP2 (20 mM Tris/HCl pH 7.8, 200 mM NaCl) followed by elution with SP3 (20 mM Tris/HCl pH 7.8, 10 mM maltose).

For GST-occludin, cells were cultivated, induced and lysed as above except that the induction time was 2 h. The fusion protein was bound to a GST affinity column (Sigma-Aldrich), washed with SP1, SP2′ (SP2, 1 mg/ml RNAse, 1 mM proteinase inhibitor; Sigma-Aldrich), SP2, eluted with SP4 (20 mM Tris/HCl pH 7.8, 2 mM glutathione), and stored at –20 °C.

For circular dichroism (CD) of occludin$^{406-521}$, MBP-occludin$^{406-521}$ was purified by amylose resin as described above followed by gel filtration (Sephadex G25; Amersham Bioscience, equilibrated with SP2). Then, 100 µg of fusion protein was incubated with 1 µg protease factor Xa (NEB, Beverly, Mass. 25 °C, 16 h). To separate MBP from the solution, amylose resin beads were added (500 µg/ml). After shaking and centrifugation (2500 × g,

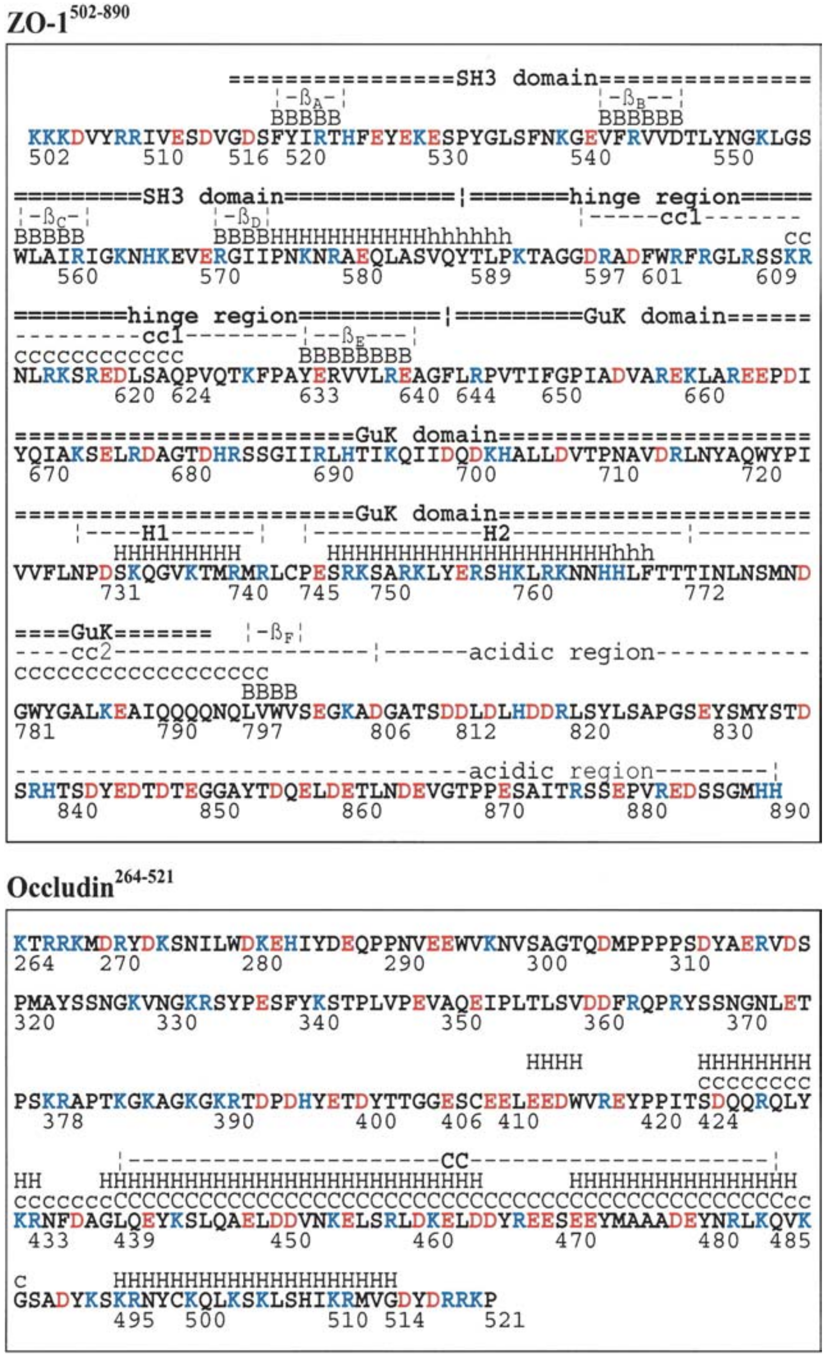

Figure 1. Amino acid sequences 502–890 of mouse ZO-1 (including the SH3-hinge-GuK unit) and 264–521 of mouse occludin (complete cytosolic C-terminal part), prediction of structural elements for potential protein-protein interactions, and derived sequence areas. Predicted secondary structural elements: H, h, α-helix; C, c, coiled-coil helix; B, β-strand (upper case means strong prediction, lower case means weaker probability). Potential binding regions defined: --cc1--, --H1--, --H2--, --cc2--, --β_{A-F}-- (β-strands adopted from SH3-hinge-GuK unit of PSD-95 [30]) from ZO-1, and --CC-- from occludin. ==SH3==, ==GuK==, ==hinge==, --acidic-- mark domains and regions, respectively, used throughout paper (for further explanations see Results). Acidic amino acids are given in red and basic ones in blue. Derived peptides: cc1 = $cc1_{37}$, ZO-$1^{597-633}$; $cc1_{29}$, ZO-$1^{597-625}$; cc2, ZO-$1^{772-806}$; H1, ZO-$1^{729-742}$; H2 = $H2_{28}$, ZO-$1^{745-772}$; $H2_{20}$, ZO-$1^{750-769}$; CC, occludin$^{439-485}$.

5 min, 20 °C), MBP and occludin$^{406-521}$ were separated as verified by SDS-PAGE (10–15%, Coomassie staining).

SPR binding studies

These were conducted on BIAcore 2000 (sensor chip CM5; Biacore, Freiburg, Germany) at 25 °C. The running buffer was 200 mM NaCl, 20 mM Tris/HCl, 50 mM $MgCl_2$, 10 mM maltose pH 7.8 (flow rate 8 µl/min). MBP fusion proteins (see above) and model peptides (see below) were immobilized (0.5–10 ng/mm^2) via coupling of primary amines according to the manufacturer's recommendations with N-hydroxysuccinimide, N-ethyl-N′(dimethylaminopropyl)-carbodiimide, and ethanolamine (Sigma-Aldrich). The interactions ZO-1/occludin or ZO-1/ZO-1 were detected through mass concentration-dependent changes of refractive index on the sensor chip and expressed as response units (RU). During association, analyte was injected for 4 min; dissociation proceeded with analyte-free running buffer for 4 min. Regeneration was achieved by washing (300 mM Na_2CO_3, 200 mM NaCl). The analyte solution was checked for non-specific binding using a non-modified reference flow cell (activated and blocked only), and comparison with standard protein mix [23]. Sensorgrams were analyzed by non-linear fitting (BIAevaluation software 3.1; Biacore). Kinetic constants were determined by local analysis of the association and dissociation phases of four to six analyte concentrations (0.25–2.5 µM) using different batches of immobilized occludin. The data were fitted to a single-site binding model (A+B→AB) which gave fits with χ^2 values <10. To estimate binding constants (K_D), association and dissociation curves were used for calculation of k_a and k_d, respectively, by means of a Langmuir isotherm (1:1 binding model).

Peptide synthesis and co-precipitation

Model peptides from mouse ZO-1 including coiled-coil or α-helical predictions ($CC1_{37}$, $H2_{20}$, $H2_{28}$, cc2; for sequences see fig. 1) were synthesized by multiple solid-phase synthesis using Fmoc chemistry [28]. For epitope mapping, $cc1_{37}$ and $H2_{28}$ were synthesized with an additional N-terminal linker of two β-alanines and a cysteine to which tetramethylrhodamine-6-maleimide (Molecular Probes Europe, Leiden, The Netherlands) was coupled.

For co-precipitation, $H2_{20}$ and $H2_{28}$ were biotinylated N-terminally and immobilized on streptavidin-agarose beads (Sigma-Aldrich). 50 µl-bead suspension equilibrated with washing buffer (100 mM NaCl, 20 mM Tris/HCl, pH 8) was incubated with 25 µl $H2_{20}$ and $H2_{28}$ (10 mg/ml, gently stirring, 3 h, 8 °C). After washing to remove unbound peptides from the solution, 125 µg/ml MBP-occludin$^{378-521}$ or GST-occludin$^{264-521}$ were incubated (16 h, 8 °C, gently stirring). Then, beads were centrifuged and washed three times; occludin trapped by immobilized peptides was eluted with SDS loading buffer (50 mM Tris/HCl pH 6.8, 100 mM dithiothreitol, 10% glycerol, 2% SDS, 0.1% bromophenol blue, 95 °C), followed by SDS-PAGE (10%) and Coomassie staining.

CD spectroscopy

CD was performed on a J-720 spectropolarimeter (Jasco, Tokyo, Japan) with ZO-1 peptides and occludin$^{406-521}$ (0.1-cm quartz cell, 185–260 nm, SP2, 25 °C). Averaged spectra of ten scans were corrected for blank and smoothed. Molar mean residue ellipticities [(θ), deg cm^2 dmol^{-1}] were calculated using molecular mass (kDa): 4.48, cc1; 3.66, $H2_{28}$; 2.76, $H2_{20}$; 3.95, cc2; 14, occludin 406–521. The secondary-structure content was determined from far UV CD spectra using the software program CDNN version 2.0c (http://bioinformatic.biochem.uni-halle.de/CD_spec/index.html) starting with a set of 33 reference proteins. The helicity f_H of peptides was determined at 222 nm by $f_H = (\theta)222 + 2340/-30300$.

Epitope mapping

Epitope mapping of predicted helical sequences of ZO-1 and occludin was performed with cellulose membrane-bound peptide arrays prepared by semi-automated spot synthesis [29]. From $cc1_{29}$, 20 different peptides out of ZO-1$^{597-625}$ were synthesized on the membrane (spots 1–20, fig. 5C), varying in sequence position and length. ZO-1$^{729-742}$ containing the proposed α-helix H1 was synthesized on the same membrane (spot 21, fig. 5C). From $H2_{20}$ (ZO-1$^{750-769}$), 120 peptides were synthesized on separate membranes (membrane not shown), differing in length and position; moreover, the epitope LRKNNHHLF (ZO-1$^{761-769}$) was subjected to substitution analysis (all amino acids replaced by all 20 coding amino acids, membranes not shown). Membranes were dried at 25 °C and washed for 10 min with methanol and 3 × 10 min with TBS (137 mM NaCl, 2.7 mM KCl, 50 mM Tris/HCl pH 8), blocked with 10% blocking solution (Sigma-Aldrich) in 50 mM Tris/HCl pH 8, 0.05% Tween 20, 10% sucrose. After washing with T-TBS (TBS, 0.05% Tween 20) membranes were incubated (gentle stirring, 4 °C, 16 h) in blocking solution with 10 µg/ml GST-occludin$^{264-521}$. Then, membranes were washed 3 × 10 min with T-TBS and incubated for 3 h with anti-GST monoclonal antibody (1:10,000, mouse; Sigma-Aldrich). Membranes were washed as before and incubated for 1.5 h with anti-mouse antibody (1:10,000) labeled with horseradish peroxidase (Sigma-Aldrich). Finally, membranes were washed 3–5× 0.5–1 h in T-TBS. GST-occludin$^{264-521}$ bound to membrane via interaction with ZO-1-peptides was quantified by enhanced chemiluminescence reagent (Amersham Biosciences) and Lumi Analyst (Boehringer, Mannheim, Germany).

From the predicted coiled-coil helical region occludin$^{439-485}$, N-terminal, middle, and C-terminal portions (each including 29 amino acids; position analysis)

were synthesized on membrane as described above. The dried membrane (25 °C) was washed for 2 min in dimethylformamide, 2 × 2 min in ethanol, 3 × 10 min with TBS, and blocked as above. After washing with T-TBS, membrane was incubated with $cc1_{37}$ (ZO-$1^{597-633}$, labeled with the red dye tetramethylrhodamine-6-maleimide, 50 µM in blocking buffer) at 4 °C overnight, and washed again. The remaining red color was quantified (LumiAnalyst), representing the amount of peptide bound. Then, the peptide library was regenerated in 6 M urea, 2 M thiourea, 1% SDS (50 °C, 30 min). After ten washings in water, the procedure was repeated with labeled $H2_{28}$ (ZO-$1^{745-772}$).

Results

Predicted binding regions

In bioinformatic studies of mouse ZO-1, coiled-coil helices were predicted as potential interaction sites in the hinge region (ZO-$1^{611-624}$) between SH3 and GuK and in the C-terminal portion of GuK (ZO-$1^{781-798}$); α-helical predictions were found in GuK (ZO-$1^{732-740}$, ZO-$1^{747-769}$) (fig. 1). The predictions agree sufficiently with structural elements in the X-ray structure of MAGuK protein PSD-95 [24], despite additional structural elements in the ZO-1 hinge and differences in amino acid sequence. Based on the homologies [24], β-strands A–F were adopted from PSD-95. Sequences containing coiled-coil and α-helical predictions were termed cc1 (ZO-$1^{597-633}$), cc2 (ZO-$1^{772-806}$), and H1 (ZO-$1^{729-742}$), H2 (ZO-$1^{745-772}$), respectively. In mouse, occludin helical structures, interrupted by short turns, were predicted in the second half of the cytosolic C-terminal tail (occludin$^{412-514}$). Within this portion, a region with helical coiled-coil character (occludin$^{424-488}$) was predicted as a potential binding site for ZO-1. The area with 100% coiled-coil probability was termed CC (occludin$^{439-485}$), and contained leucine heptad motifs, one of the properties of coiled-coils. Within cc1 and cc2 of ZO-1, coiled-coil patterns were recognized only when the search window was shortened to 14 amino acids. This means coiled-coil properties were detected for short sequence patches only. The probability of coiled-coil prediction was >60% within cc1 and >90% within cc2, indicating, at least, a propensity for coiled-coil conformation. ZO-1 sequences cc1 with a weak coiled-coil prediction, and H1 and H2 with an α-helix prediction are dominated by basic amino acids; in the occludin strong coiled-coil prediction CC, acidic residues predominate (for exact amino acid order of predictions and defined sequences see fig. 1).

Binding segments detected in ZO-1 and occludin

Based on the bioinformatic data, parts of ZO-1 and occludin were expressed as an MBP fusion protein and their interaction was measured by SPR. Figure 2 A shows typical sensorgrams of selected ZO-1 fragments, differing considerably in binding elements and binding efficiency under identical conditions, with immobilized occludin. ZO-$1^{589-772}$ (hinge ~ GuK without cc2) exhibited the strongest, ZO-$1^{644-812}$ (GuK ~ β-strand F ~ begin of acidic region) moderate, and ZO-$1^{644-731}$ (N-terminus of GuK without helices) neglegible binding. Thus, the relevance of the predicted interaction areas can be verified

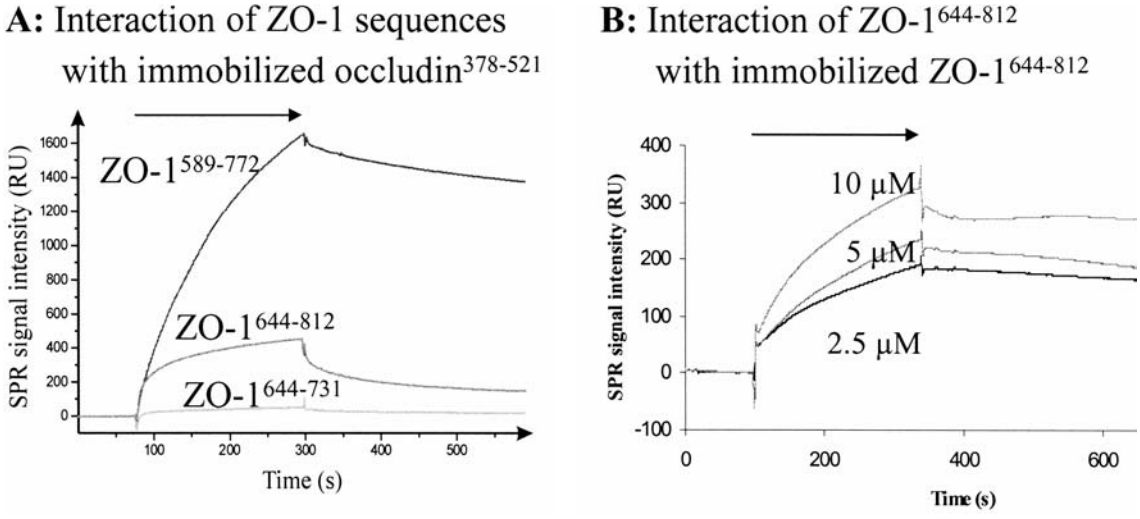

Figure 2. Representative sensorgrams of SPR showing the association and dissociation of fragments from ZO-1 with and from cytosolic C-terminal segments of occludin (*A*) and ZO-1-fragments (*B*). (*A*) Strongly (hinge-GuK without cc2), moderately (complete GuK), and weakly (GuK without H1, H2, cc2) binding ZO-1 sequences (2.5 µM each) infused onto immobilized occludin (10 ng/mm^2). For definition of H1, H2, and cc2 see the legend to figure 1. (*B*) Concentration-dependent interaction of a selected GuK segment from ZO-1 with the same segment immobilized (7.4 ng/mm^2). RU, resonance units. Arrows mark infusion interval of the ZO-1 protein accompanied by association, followed by the dissociation interval; MBP fusion proteins were used.

by SPR data. The opposite approach, binding of occludin to ZO-1, was also performed. The binding constants (K_D), e.g, for MBP-occludin$^{378-521}$ superfused over the immobilized sequences cc1$_{37}$, H_{20}, and H_{28} of ZO-1 were 460 ± 104, 76 ± 32, and 58 ± 20 nM, respectively (mean ± SE, n ≥ 4). For immobilized cc2 of ZO-1, no reasonable interaction constants with occludin could be calculated.

Figure 3A shows relative binding efficiencies of ZO-1 constructs to the immobilized cytosolic C-terminal part of occludin. Maximum binding was found with ZO-1$^{589-772}$ (hinge region containing cc1 + GuK, but without cc2). The association decreased by 17% after N-terminal truncation (ZO-1$^{597-772}$), by 45% after further truncation (ZO-1$^{601-772}$), and by 80% after exclusion of cc1 (shortening up to the N terminus of GuK; ZO-1$^{644-772}$). Compared to the best binding sequence, the binding was 74% lower after C-terminal prolongation of GuK by cc2, β-strand F, and the beginning of the acidic region (ZO-1$^{644-812}$). The N-terminal half of GuK (ZO-1$^{644-731}$; without H1, H2, cc2) and the GuK domain C-terminally prolonged by the acidic region (ZO-1$^{644-890}$) showed very low binding (fig. 3A). Sequences containing SH3, hinge, and GuK (e.g., ZO-1$^{502-812}$, ZO-1$^{502-772}$) bound moderately, whereas constructs with PDZ3 and SH3 (ZO-1$^{413-619}$) did not associate at all (data not shown). We conclude that SH3 of ZO-1 is not directly involved in the interaction. Figure 3B shows the highest binding efficiency of ZO-1 when occludin was N-terminally shortened to that area including the predicted helical sequences (occludin$^{406-521}$). The results indicate that, in ZO-1, the hinge region with a predicted coiled-coil helix and parts of the GuK domain with α-helical prediction interact with the helical portion in occludin. To confirm structural elements identified by SPR measurements, peptides derived from H2 of GuK were tested by an independent method. In co-precipitation experiments, both GST- and MBP-fusion proteins of occludin$^{264-521}$ were found to associate with peptide sequences from H2 immobilized on beads. This is demonstrated by detection of the fusion proteins in precipitates of H2-carrying beads; no occludin was detectable in the bead-free supernatant. Peptide $H2_{28}$ (with two basic amino acids more than $H2_{20}$) bound occludin more effectively than did peptide $H2_{20}$. With H2-free beads, occludin remained in the soluble fraction and was not visible in precipitate (blots not shown).

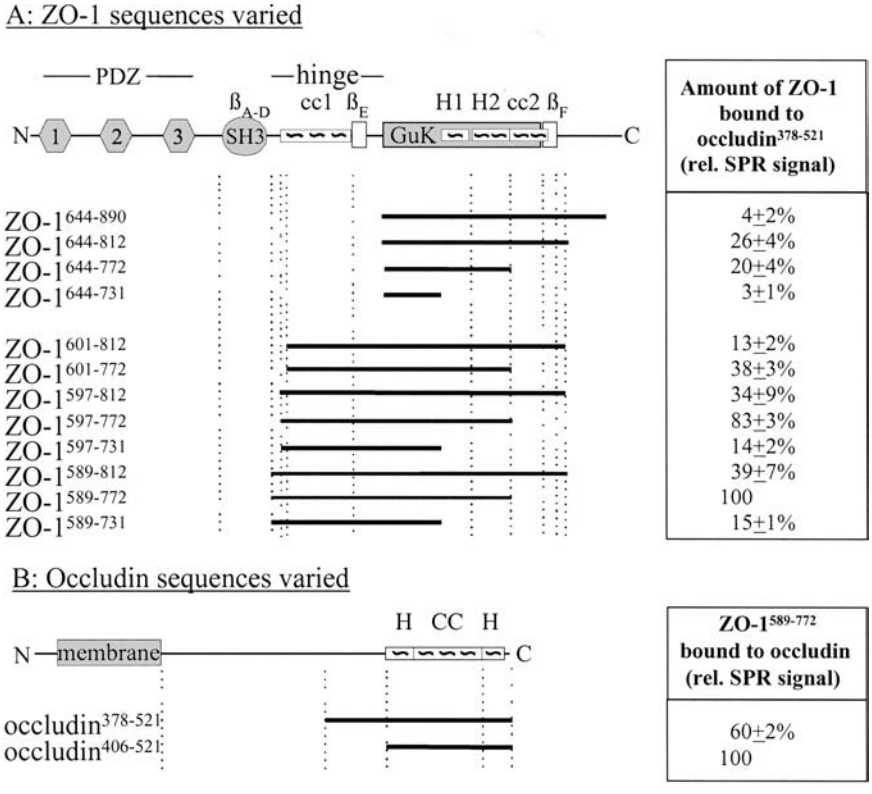

Figure 3. Protein binding efficacy of fragments from ZO-1 with cytosolic C-terminal segments of occludin detected by SPR: binding amounts of ZO-1 constructs differing in length and position onto immobilized occludin (*A*) and adherence of ZO-1$^{589-772}$ to immobilized occludin segments varying in length (*B*). For abbreviations and sequence names see figure 1 and its legend. Data represent the maximum amount of a protein bound (SPR signal intensity) registered 4 min after superfusion with 2.5 µM, normalized to the level of occludin immobilized. For comparison of different constructs, binding values were related to the value of that sequence of a series of experiments showing the strongest association. MBP fusion proteins were used. Data are given in % and are the mean ± SE, n ≥ 4.

In addition, a concentration-dependent association between GuK domains of ZO-1 was demonstrated. Thus, the infusion, e.g., of 10 µM ZO-$1^{644-812}$ onto immobilized ZO-$1^{644-812}$ led to the binding of 320 RU/4 min (fig. 3B). Self-association was further indicated by the finding that greater amounts of GuK-containing constructs were bound (e.g., 450 RU/4 min of 2.5 µM ZO-$1^{378-521}$) when occludin$^{378-521}$ was immobilized than vice versa (only 100 RU/4 min of 2.5 µM occludin$^{378-521}$ bound to ZO-$1^{644-812}$).

Helical properties of fragments involved in the interaction of ZO-1 and occludin

CD experiments indicated predominantly helical secondary-structure elements of occludin$^{406-521}$ in buffer (60% helicity). Spectra with a maximum at 195 nm and double minima at 209 and 222 nm are characteristic for α-helices (fig. 4A). For spectra of peptides cc1, H2 and cc2 of ZO-1 see figure 4B–D. cc1 and cc2 were less structured in buffer (5–8% helicity for 222 nm), but their helical propensity increased after addition of TFE (a helix-promoting reagent) to 14% for cc1, 15% for $H2_{20}$, and 60% for $H2_{28}$. cc2 (ZO-$1^{772-806}$) revealed in buffer characteristic α-helical structure (78%) improving to 94% under TFE. The minima at 209 and 222 nm were overlapped by a third minimum at 217 nm which is typical for a β-strand (in cc2 β_F, ZO-$1^{797-800}$) contributing to the structure.

Contribution of peptide sequences predicted as α- or coiled-coil helix to the interaction between ZO-1 and occludin

To characterize a binding motif within the identified binding sequences, different peptides, spotted on a membrane, were tested for the association of occludin and ZO-1 segments. $cc1_{29}$ fragments showed ≥69% binding of GST-occludin$^{264-521}$ if at least one leucine heptad motif plus at least five basic amino acids, near to the two N-terminal leucines, were present. When cc1 peptides containing either the N-terminal or the C-terminal leucine heptad were compared, the latter seemed to be less relevant

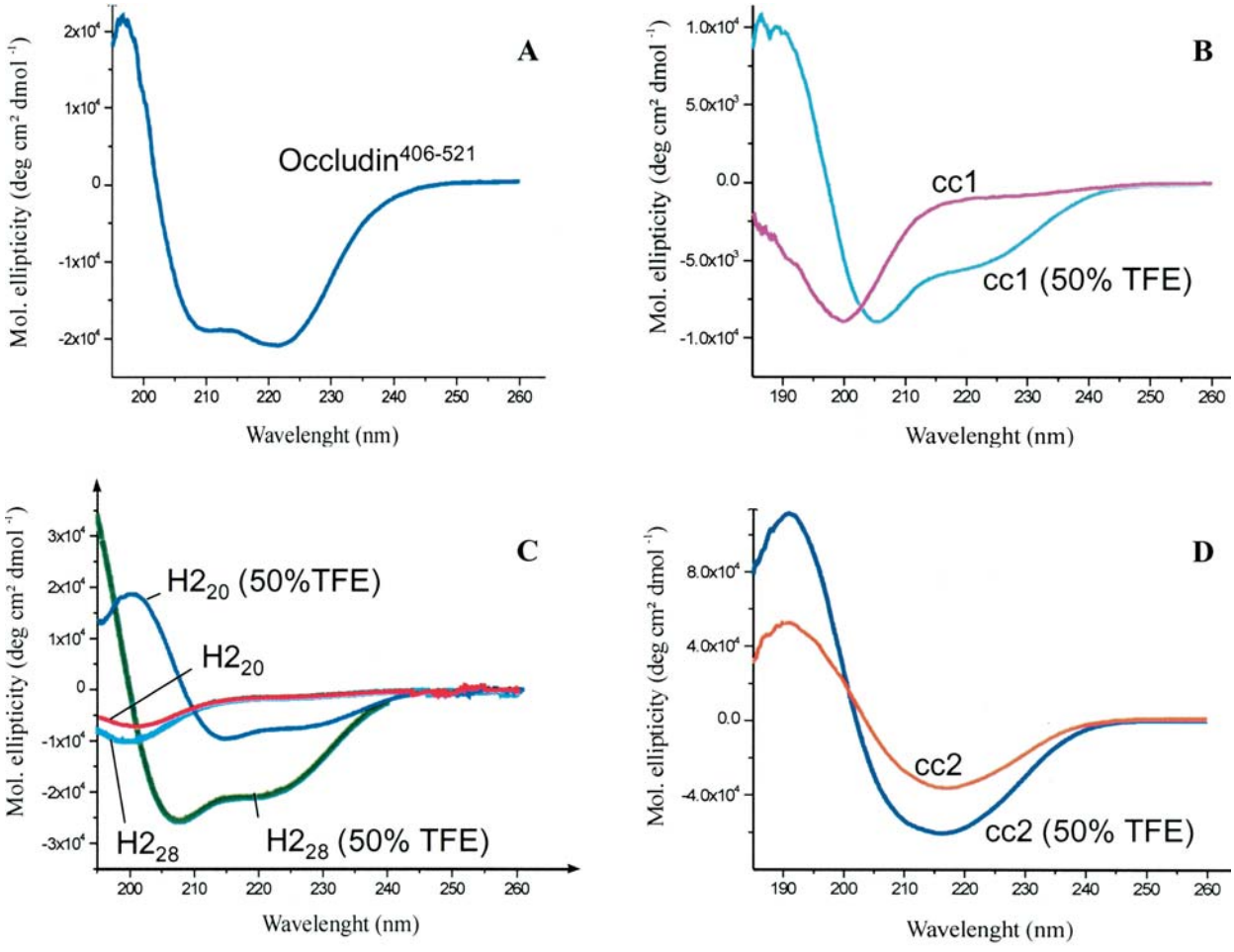

Figure 4. CD spectra of occludin$^{406-521}$, and peptides cc1, H2, cc2 from ZO-1; average of ten scans with background substracted. (*A*) Cytosolic C-terminal occludin$^{406-521}$ (8 µM, free of MBP) shows a typical α-helical character in buffer (60% helicity). (*B–D*) 50 µM cc1, $H2_{20}$, $H2_{28}$, cc2 in buffer and 50% trifluorethanol (TFE a helix-promoting agent). Helical characteristics measured in the presence of TFE: cc1, 14%; H2, up to 60%, cc2, 94% helix propensity (for further details see Results). For peptide sequences see legend to figure1.

for occludin binding if it did not contain enough basic residues (fig. 5A, spots 1–20). Compared with cc1, peptide comprising the predicted α-helical region H1 from the GuK domain exhibited 41% binding with occludin$^{264-521}$ (fig. 5B, spot 21). Note that H1 also has a surplus of basic residues.

Comparing the amount of occludin$^{264-521}$ bound to peptides from $H2_{20}$ (ZO-1$^{750-769}$) differing in position and length, one can see that the binding center was within L^{754}YERSHKL^{761}RKNNHHL^{768}. However, the hydrophobic leucine heptad motifs were not essential for the association. To assure >50% binding, the middle leucine flanked by at least five basic amino acids was necessary (fig. 6, left). Substitution analysis of L^{761}RKNNHHL^{768} (replacement of each amino acid by all others) revealed that occludin binding is considerably reduced when R^{762} was replaced by any other amino acid except lysine. All other amino acids of the peptide can be replaced by almost any other amino acid without noticeable changes in binding, except substitution with negatively charged glutamate and aspartate, which decreased the signal intensity (data not shown). Peptides from the N-terminal tail of $H2_{20}$ (containing glutamate and, at the most, three or four basic residues only) showed no association (fig. 6, right). In occludin, sequence analysis of the strongly predicted coiled-coil region CC (occludin$^{439-485}$) revealed a triple leucine heptad pattern and, shifted by three residues, another hydrophobic heptad motif. CC contains 15 acidic but only 7 basic amino acids. Almost all the acidic residues flank hydrophobic ones and the majority of acidic residues are localized C-terminally from the coiled-coil region. Association measurements with N-ter-

A

Spot	Amino acid sequences out of $cc1_{29}$ (ZO-1$^{597-625}$) including predicted coiled coil-helix	Occludin bound
12	DRA DFWRFRG **L**RSSKRN **L**RKSRED LS	100 %
13	DRA DFWRFRG **L**RSSKRN **L**RKSR	97±2%
1	DRA DFWRFRG **L**RSSKRN **L**RKSRED LSAQP	93±3%
7	G **L**RSSKRN **L**RKSRED LSAQP	93±4%
6	WRFRG **L**RSSKRN **L**RKSRED LSAQP	92±6%
4	DFWRFRG **L**RSSKRN **L**RKSRED LSAQP	91±2%
18	G **L**RSSKRN **L**RKSRED LS	90±5%
5	FWRFRG **L**RSSKRN **L**RKSRED LSAQP	82±5%
3	A DEWRFRG **L**RSSKRN **L**RKSRED LSAQP	81±3%
2	RA DFWRFRG **L**RSSKRN **L**RKSRED LSAQP	79±5%
19	SSKRN **L**RKSRED LS	78±2%
14	DRA DFWRFRG **L**RSSKRN **L**R	76±7%
20	G **L**RSSKRN **L**RKSR	70±9%
8	SSKRN **L**RKSRED LSAQP	69±3%
15	DRA DFWRFRG **L**RSSK	43±6%
16	DRA DFWRFRG **L**R	37±8%
17	DRA DFWRFR	23±2%
9	N **L**RKSRED LSAQP	9±1%
10	KSRED LSAQP	5±2%
11	D LSAQP	2±1%

B

	Peptide sequence H1 (ZO-1$^{729-742}$) including a predicted α-helix	
21	NPDS KQGVKRM RMR	41±2%

C

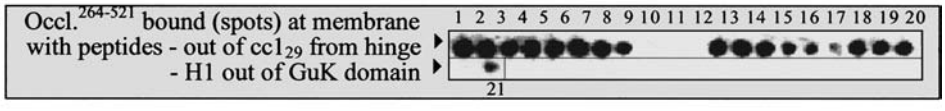

Figure 5. Epitope mapping analysis of helix-containing peptide sequences $cc1_{29}$ and H1 from ZO-1 found to associate with occludin. The association of GST-occludin$^{264-521}$ was measured on peptide libraries with fragments out $cc1_{29}$ (ZO-1$^{597-625}$, within the hinge region located between SH3 and GuK) and on H1 (ZO-1$^{729-742}$, sequence of the GuK domain). C-termini of the peptides were immobilized on a membrane and bound GST-occludin protein was visualized as chemiluminescence via peroxidase-labeled anti-GST antibodies. The light signal is shown inversely, and the darkest spot, therefore, represents the strongest binding. Chemiluminescence was expressed in % related to that spot showing the best binding within a series of experiments. (*A*) GST-occludin binding to $cc1_{29}$. $cc1_{29}$ includes a leucine (bold) heptad motif within which a coiled-coil helix was predicted as described in the text. $cc1_{29}$ was varied in 3-amino acid steps (length and position analysis). (*B*) GST-occludin binding to peptide H1, within which a coiled-coil helix was predicted (for predictions see fig. 1). (*C*) Representative membrane with cc1 and H1 peptides immobilized after incubation and visualization. Data are the mean ± SE, n = 4.

Spot	Sequences out of $H2_{20}$ (ZO-$1^{750-769}$)	Occl. bound	Spot	Sequences out of $H2_{20}$	Occl. bound
1	SARK LYERSHK LRKNNHH LF	72±11%	67	SARK LYERS	4± 2%
20	LYERSHK LRKNNHH L	67± 7%	70	K LYERSHK L	3± 1%
15	LYERSHK LRKNNHH LF	56±15%	82	K LYERSHK	1± 1%
2	SARK LYERSHK LRKNNHH L	52±10%	83	LYERSHK L	2± 1%
36	RSHK LRKNNHH LF	69± 7%	84	YERSHK LR	2± 1%
21	YERSHK LRKNNHH LF	63±18%	92	SARK LYE	1± 1%
55	HK LRKNNHH LF	57± 8%	95	K LYERSH	1± 1%
19	K LYERSHK LRKNNHH	57±15%	96	LYERSHK	1± 1%
39	RK LYERSHK LRK	57±20%	106	SARK LY	1± 1%
76	HK LRKNNHH	66±20%	107	ARK LYE	4± 2%
75	SHK LRKNNH	56±15%	110	LYERSH	2± 1%
42	YERSHK LRKNNH	53±13%	111	YERSHK	2± 1%

Figure 6. Epitope mapping analysis of α-helical peptide sequence $H2_{20}$ (ZO-$1^{750-769}$, from the GuK domain of ZO-1) with respect to binding to GST-occludin$^{264-521}$. $H2_{20}$ was varied in 1-amino acid steps (length and position analysis); only the strongest (left) and weakest (right) binding sequences are shown. Membranes are not shown; mean ± SE, n = 4. For predictions see figure 1 and for further conditions see figure 5.

Spot	Peptide sequences out of coild coil-helix CC in occludin's C-terminus (occludin$^{439-484}$)	$cc1_{37}$ bound	$H2_{28}$ bound
5	E **L**SRLDKE **L**DDYREE SEEYMAA ADEYNRL	100%	100%
6	**L**SRLDKE **L**DDYREE SEEYMAA ADEYNRL K	73%	96%
3	**L**DDVNKE **L**SRLDKE **L**DDYREE SEEYMAA A	30%	58%
4	DDVNKE **L**SRLDKE **L**DDYREE SEEYMAA AD	27%	50%
1	LQE YKSLQAE **L**DDVNKE **L**SRLDKE **L**DDYR	15%	17%
2	QE YKSLQAE **L**DDVNKE **L**SRLDKE **L**DDYRE	15%	19%

Figure 7. Epitope mapping analysis of selected peptides from the coiled-coil helix-containing domain CC from the cytosolic C-terminal end of occludin, association with peptides $cc1_{37}$ or $H2_{28}$ of ZO-1 within which helices were predicted. $cc1_{37}$ (ZO-$1^{597-633}$, from the hinge region located between SH3 and GuK) and $H2_{28}$ (ZO-$1^{745-772}$, from GuK) were incubated on membranes with fragments from occludin$^{439-484}$ including segments with coiled-coil prediction. N-terminal, middle, and C-terminal portions of occludin$^{439-484}$ were covalently bound to the membrane (latter not shown). Bold L marks leucine heptad motifs of the predicted coiled-coil helical area. $cc1_{37}$ and $H2_{28}$ were labeled with tetramethylrhodamine. The amount of peptide molecules bound was visualized via light absorbance of the label, expressed in % of that sequence showing maximum binding. For predictions see figure 1; for further details see figure 5.

minal, middle, and C-terminal portions of the leucine heptad area demonstrated that, in the C-terminal half, one leucine heptad and at least three hydrophobic residues are essential for >70% binding of ZO-1 peptides $cc1_{37}$ and $H2_{28}$. If the strongly acidic C-terminus was absent, less than 20% binding was registered (fig. 7).

Discussion

This work has identified molecular regions and mechanisms of interaction between murine ZO-1 and occludin significantly regulating the structure and function of TJs. A similar gradation of binding strength for distinct ZO-1 fragments was found by independent techniques, such as SPR and epitope mapping. Both methods reveal strong association of cc1- and H2-containing segments from ZO-1 with occludin. SPR with fragments both possessing and lacking additional proteins led to comparable results. Identical results were also obtained with MBP- and GST-occludin in pull-down and peptide mapping assays using immobilized peptides from ZO-1. This further supports the applicability of SPR and epitope mapping to studying the occludin-ZO-1 interaction. A considerable influence of MBP, applied in SPR studies, is excluded as MBP alone associates neither with itself nor with ZO-1 or occludin [23]. On the other hand, steric hindrance by the large size of MBP or GST could limit the accessibility of smaller fused constructs. However, hindrance should be diminished by the spacer of 15–20 amino acids introduced between the peptide and MBP. For GST, caution is needed as GST fusion proteins can oligomerize [30]. GST, therefore,

has not been used in SPR but mainly in mapping studies, as a marker for the C-terminal 258-amino acid protein of occludin. Interacting concentrations and binding constants of ZO-1 and occludin were found to be in the submicromolar range, pointing to a strong and reversible interaction. Such interactions are expected to be of regulatory relevance and might allow occludin to modulate ZO-1 to constitute the protein complex of TJ.

Earlier, an association of the cytosolic C-terminal tail of occludin and the GuK domain of ZO-1 was indicated [10, 15]. This and our bioinformatic studies led us to a helical interaction hypothesis [23]. As potentially interacting domains in ZO-1, we considered sequences possibly forming coiled-coil helices cc1 and cc2, and α-helices H1 and H2. The binding areas are found not only in the GuK domain of ZO-1 as proposed earlier [10] but, interestingly, also within the hinge region (cc1) connecting the SH3 and GuK domain. In occludin, α- and coiled-coil helices are predicted within the last 109 C-terminal amino acids. A construct comprising this region (occludin$^{406-521}$) does indeed show better binding in SPR studies than longer ones (e.g., occludin$^{378-521}$). The association is probably due to the highly acidic sequence 439–485 representing the strongest coiled-coil prediction in occludin. In contrast, the C-terminal following helix is strongly basic which would repulse the basic regions of the hinge-GuK area. Human occludin$^{440-469}$ corresponding to mouse occludin$^{439-468}$ with 90% homology has been proposed to interact with ZO-1 in a peptide bait study using membrane fractions from polarized T84 cell monolayers [31]. Our SPR binding studies provide evidence that the sequence with coiled-coil propensity cc1 (in the hinge region localized between SH3 and GuK) and α-helical portions H1 and H2 (within GuK) are essential for the association in ZO-1. The hinge region has not previously been considered as an interaction site. In peptide studies, the binding intensity of H2 appears stronger than that of cc1 and is lowest with H1. This agrees with the better helical propensity of H2 than of cc1, measured as peptides by CD, and corresponds to the number of positively charged residues essential for optimal attraction of the negative occludin helices. In epitope mapping of free peptides, however, sequences can be displaced from their tertiary structure. This might be problematic for correct folding and could result in overestimation of hydrophobic interactions. The same restriction is given for structures of free peptides when detected by CD in the presence of TFE. Thus, e.g., the helical nature of cc1 alone is not expected in the environment of the cell cytoplasm. However, helix formation appears possible after interaction with another helix, such as CC of occludin. Moreover, limits of peptide studies have to be considered for occludin also. The tertiary structure of its binding domain has not been completely solved and no crystallographically solved analogues are available. Nevertheless, the peptide data are supported by the SPR measurements with recombinant proteins, showing better occludin association when all three ZO-1 elements are present than in the absence of single elements, e.g., of cc1.

In contrast, the GuK C-terminal helix cc2 was not confirmed as a binding element. The peptide cc2 (ZO-1$^{772-806}$) includes β-strand F, adopted from the synaptic membrane protein PSD-95 [24], and its C-terminus overlaps with the acidic region. cc2 reduces occludin binding in those constructs containing cc1. The surplus of acidic residues in cc2, in the case of isolated constructs, could favor adherence to the basic helix cc1, thus blocking interaction of cc1 with acidic helix CC (occludin$^{439-485}$). The interference by cc2 disappears when expressed together with SH3, the hinge region and GuK. Here cc2 is obviously separated from cc1 and, hence, from the binding center. This agrees with the crystal structure of PSD-95, another MAGuK protein. In PSD-95, SH3 and GuK form a structural unit stabilized via interaction of β-strands in SH3 (β_{A-D}), preceding (β_E) and after (β_F) GuK [24, 25]. The sequential order of MAGuK domains is highly conserved [5]. For ZO-1, therefore, we postulate a SH3-GuK unit with a specific hinge in between, from which, via the β-strand components, cc2 is kept away from the occludin binding area.

Constructs of GuK prolonged by the acidic region, following the C-terminus of GuK (ZO-1$^{806-890}$), but without SH3, show still lower binding to occludin than the complete GuK domain alone. The acidic region is assumed to have the potential to interfere with the interaction between basic GuK parts and the occludin acidic helix. The acidic region of ZO-1 as well as the acidic CC helix of occludin contain highly conserved and, in part, potentially phosphorylated tyrosines next to the acidic amino acids. Tyrosine phosphorylation would strengthen the negative charges and could sterically affect helical interaction. These considerations are in agreement with reduced binding of ZO-1 to occludin observed after unspecific tyrosine phosphorylation of occludin [32] or both proteins [33]. However, exact phosphorylation positions still need to be identified.

Our binding studies with peptide libraries from regions, confirmed in protein-binding studies, with coiled-coil and α-helical predictions suggest hydrophobic and ionic interactions. For cc1, G **L**RSSKRN **L**RKSR (ZO-1$^{606-618}$) is identified as the core binding region. It contains the consensus LRxS repeating twice and LRxXxR (x, variable; X, non-charged). The leucine heptad motif (bold) is indicated as a potential coiled-coil helix if the algorithm of Lupas [27] with a 14-amino acid recognition window is applied. Moreover, basic amino acids (underlined) following the leucines are also necessary for binding. We conclude that basic arginines in consensus positions are involved in ionic association of acidic helices in occludin and stabilize the helix-helix interaction. The

core region in H2 is HK LRKNNH (ZO-1$^{759-766}$) also dominated by basic residues flanking a leucine. H2 showed helical propensity in solution with TFE which agrees with the helix found in a crystallographically solved analogue [24]. The position of uncharged and apolar amino acids in H2 is typical for α-helices [34], thus serving as a hydrophobic anchor. But ionic binding also plays a specific role, as supported by epitope mapping. Fragments without the pattern HKLRKXxH do not attract occludin strongly. R^{762} is especially relevant because, after substitution by non-basic or acidic amino acids, the binding to the negatively charged occludin portion is strongly reduced. cc1 and H2 share a very similar peptide pattern R/HxLRxXxR/H. In a helical conformation [34], this pattern results in hydrophobic anchors on one phase and massive basic charges on the other phase of the helix. In occludin, the core binding region E **L**SRLDKE **L**DDYREE SEEY (occludin$^{455-473}$) shows a two to three leucine motif (bold) and excess of acidic residues. The relevance of this leucine motif agrees with our concept that the C-terminal cytosolic part of occludin regulates its association to TJs through a coiled-coil domain as proposed for human occludin (L^{440}–E^{469}). The latter includes a part of the core region identified by us, has been proven α-helical, and may interact with other helices [31]. A suitable binding sequence in occludin is ELxDXxE which complements the consensus pattern R/HxLRxXR/H in cc1 and H2 of ZO-1. Thus, the specificity of the interaction to ZO-1 is probably caused by the acidic residues in occludin fitting perfectly to the basic helices on ZO-1. Our data, therefore, demonstrate that ZO-1 and occludin associate via helix-helix interaction stabilized by coiled-coil helices and specific ionic links.

The concept of an SH3-GuK unit in ZO-1 connected by the specific hinge, as suggested by our findings, is supported by yeast two-hybrid screens with several MAGuKs. Thus, Dlg [26], CASK [35], chapsyn-110 [36], and SAP-97 [37] show intramolecular interaction between their SH3 and GuK. The hinge region in MAGuKs differs considerably in sequence and length. In ZO-1, the occludin-binding core of the hinge includes two adjacent serines recognized as a phosphorylation site [38], further supporting regulatory relevance. Phosphorylation would weaken the overall positive charge of the hinge, which, in turn, would diminish interaction with negatively charged binding sites in occludin. Hinge regions of MAGuKs are often the target of regulatory adaptor proteins like calmodulin for SAP-102 [39] or protein 4.1 for Dlg [37]. Upon adaptor binding, swapping of SH3 and GuK has been suggested, enabling dimerization of MAGuKs in which an intermolecular SH3-hinge-GuK unit is formed [24]. Interestingly, our experimentally identified occludin-binding site in ZO-1, cc1, is exactly located within its hinge region. Occludin, therefore, might induce in ZO-1, especially in the hinge featuring coiled-coil propensity, a conformational shift that facilitates interactions with the CC domain of occludin. Taken together, we conclude that occludin is an adaptor protein for ZO-1 possibly influencing dimerization of the latter.

For the first time, we demonstrate that a sequence of ZO-1 including the GuK domain (ZO-1$^{644-812}$) associates with another free GuK. This is a new possibility of MAGuK-MAGuK interaction, additional to the intermolecular SH3-GuK binding postulated for MAGuK protein PSD-95 [24]. For ZO-1, it means that one of its domains for occludin binding is able to dimerize. The complex of ZO-1 and occludin, hence, could form a heterodimer or heterooligomer. On the other hand, helical structures of occludin could compete with GuK-GuK interactions (at least in terms of helix-helix association) and, hence, would counteract oligomerization. However, for full-length ZO-1, a GuK-GuK separating effect is opposed by SH3. In MAGuK-MAGuK interaction, SH3 of one molecule is assumed to associate with GuK of another molecule via β-sheet formation [24]. Potential ZO-1 oligomerization is further supported by our finding of higher ratios of GuK-containing constructs bound to immobilized occludin than found vice versa.

In conclusion, the interaction mechanisms including exact binding areas between ZO-1 and occludin were identified as the hinge region and GuK domain of ZO-1 and the coiled-coil domain near the occludin C-terminus. Despite the fact that ZO-1 recruits the majority of TJ proteins, we have demonstrated that it may oligomerize itself which is a new possibility for the formation of the TJ complex. The area of ZO-1 for oligomerization and for binding of occludin is the same. Moreover, the assumption is supported that the SH3 and GuK domains form, via the hinge region, an integrated functional unit in ZO-1. As this unit is modified by the TJ-specific protein occludin, the identified interactions are thought to be of relevance for the formation of the multiprotein complex of TJs. Thus, the regulation of the intermolecular interaction between SH3-hinge-GuK units by occludin is thought to be a new principle supporting the scaffolding role of ZO-1 in the arrangement of the TJ network.

Acknowledgments. The authors thank Dr. J. Selfe for preparation of the manuscript and Gislinde Hartmann for technical assistance; support: DFG BL308/6-1, SFB507 A2.

1 Balda M. S., and Matter K. (1998) Commentary – tight junctions. J. Cell Sci. **111:** 541–547
2 Stevenson B. R. and Keon B. H. (1998) The tight junction: morphology to molecules. Annu. Rev. Cell Dev. Biol. **14:** 89– 109
3 Tsukita S. and Furuse M. (2001) Multifunctional strands in tight junctions. Nat. Rev. Mol. Cell Biol. **2:** 285–293
4 Gonzalez-Mariscal L., Betanzos A., Nava P. and Jaramillo B. E. (2003) Tight junction proteins. Prog. Biophys. Mol. Biol. **81:** 1–44

5 Gonzalez-Mariscal L., Betanzos A. and Avila-Flores A. (2000) MAGUK proteins: structure and role in the tight junction. Semin. Cell Dev. Biol. **11:** 315–324

6 McGee A. W. and Bredt D. S. (1999) Identification of an intramolecular interaction between the SH3 and guanylate kinase domains of PSD-95. J. Biol. Chem. **274:** 17431–17436

7 Woods D. F., Hough C., Peel D., Callaini G., and Bryant P. J. (1996) Dlg protein is required for junction structure, cell polarity, and proliferation control in *Drosophila* epithelia. J. Cell Biol. **134:** 1469–1482

8 Kim E., Naisbitt S., Hsueh Y. P., Rao A., Rothschild A., Craig A. M. et al. (1997) GKAP, a novel synaptic protein that interacts with the guanylate kinase-like domain of the PSD-95/SAP90 family of channel clustering molecules. J. Cell. Biol. **136:** 669–678

9 Bazzoni G., Martinez-Estrada O. M., Orsenigo F., Cordenonsi M., Citi S. and Dejana E. (2000) Interaction of junctional adhesion molecule with the tight junction components ZO-1, cingulin, and occludin. J. Biol. Chem. **275:** 20520–20526

10 Fanning A. S., Jameson B. J., Jesaitis L. A. and Anderson J. M. (1998) The tight junction protein ZO-1 establishes a link between the transmembrane protein occludin and the actin cytoskeleton. J. Biol. Chem. **273:** 29745–29753

11 Itoh M., Nagafuchi A., Moroi S. and Tsukita S. (1997) Involvement of ZO-1 in cadherin-based cell adhesion through its direct binding to α catenin and actin filaments. J. Cell Biol. **138:** 181–192

12 Itoh M., Morita K. and Tsukita S. (1999) Characterization of ZO-2 as a MAGUK family member associated with tight as well as adherens junctions with a binding affinity to occludin and alpha catenin. J. Biol. Chem. **274:** 5981–5986

13 Wittchen E. S., Haskins J. and Stevenson B. R. (1999). Protein interactions at the tight junction – actin has multiple binding partners, and ZO-1 forms independent complexes with ZO-2 and ZO-3. J. Biol. Chem. **274:** 35179–35185

14 Furuse M., Fujita K., Hiiragi T., Fujimoto K. and Tsukita S. (1998) Claudin-1 and -2: novel integral membrane proteins localizing at tight junctions with no sequence similarity to occludin. J. Cell Biol. **141:** 1539–1550

15 Furuse M., Itoh M., Hirase T. Nagafuchi A., Yonemura S., Tsukita S. et al. (1994) Direct association of occludin with zo-1 and its possible involvement in the localization of occludin at tight junctions. J. Cell Biol. **127:** 1617–1626

16 Furuse M., Hirase T., Itoh M., Nagafuchi A., Yonemura S., Tsukita S. et al. (1993) Occludin – a novel integral membrane-protein localizing at tight junctions. J. Cell Biol. **123:** 1777–1788

17 Bamforth S. D., Kniesel U., Wolburg H., Engelhardt B. and Risau W. (1999) A dominant mutant of occludin disrupts tight junction structure and function. J. Cell Sci. **112:** 1879–1888

18 Balda M. S., Whitney J. A, Flores C., Gonzales S., Cereijido M. and Matter K. (1996) Functional dissociation of paracellular permeability and transepithelial electrical resistance and disruption of the apical-basolateral intramembrane diffusion barrier by expression of a mutant tight junction membrane protein. J. Cell Biol. **134:** 1031–1049

19 Wong V. and Gumbiner B. M. (1997) A synthetic peptide corresponding to the extracellular domain of occludin perturbs the tight junction permeability barrier. J. Cell Biol. **136:** 399–409

20 Van Itallie C. M. and Anderson J. M. (1997) Occludin confers adhesiveness when expressed in fibroblasts. J. Cell Sci. **110:** 1113–1121

21 Lacaz-Vieira F., Jaeger M. M., Farshori P. and Kachar B. (1999) Small synthetic peptides homologous to segments of the first external loop of occludin impair tight junction resealing. J. Membr. Biol. **168:** 289–297

22 Ryeom S. W., Paul D. and Goodenough D. A. (2000) Truncation mutants of the tight junction protein ZO-1 disrupt corneal epithelial cell morphology. Mol. Biol. Cell **11:** 1687–1696

23 Schmidt A., Utepbergenov D. I., Krause G. and Blasig I. E. (2001) Use of surface plasmon resonance for real-time analysis of the interaction of ZO-1 and occludin. Biochem. Biophys. Res. Commun. **288:** 1194–1199

24 McGee A. W., Dakoji S. R., Olsen O., Bredt D. S., Lim W. A. and Prehoda K. E. (2001) Structure of the SH3-guanylate kinase module from PSD-95 suggests a mechanism for regulated assembly of MAGUK scaffolding proteins. Mol. Cell **8:** 1291–1301

25 Tavares G. A., Panepucci E. H. and Brunger A. T. (2001) Structural characterization of the intramolecular interaction between the SH3 and guanylate kinase domains of PSD-95. Mol. Cell **8:** 1313–1325

26 Nix S. L., Chishti A. H., Anderson J. M. and Walther Z. (2000) hCASK and hDlg associate in epithelia, and their Src homology 3 and guanylate kinase domains participate in both intramolecular and intermolecular interactions. J. Biol. Chem. **275:** 41192–41200

27 Lupas A. (1996) Prediction and analysis of coiled-coil structures. Methods Enzymol. **266:** 513–525

28 Janek K., Rothemund S., Beyermann M., Zipper J., Fabian H., Bienert M. et al. (2001) Study of the conformational transition of A beta(1–42) using D-amino acid replacement analogues. Biochemistry **40:** 5457–5463

29 Frank R. and Overwin H. (1996) SPOT synthesis: epitope analysis with arrays of synthetic peptides prepared on cellulose membranes. Methods Mol. Biol. **66:** 149

30 Maru Y., Afar D. E., Witte O. N. and Shibuya M. (1996) The dimerization property of glutathione S-transferase partially reactivates Bcr-Abl lacking the oligomerization domains. J. Biol. Chem. **271:** 15353–15357

31 Nusrat A., Chen J. A., Foley C. S., Liang T. W., Tom J., Cromwell M. et al. (2000) The coiled-coil domain of occludin can act to organize structural and functional elements of the epithelial tight junction. J. Biol. Chem. **275:** 29816–29822

32 Kale G., Naren A. P., Shet P. and Rao R. K. (2003) Tyrosine phosphorylation of occludin attenuates its interactions with ZO-1, ZO-2, and ZO-3. Biochem. Biophys. Res. Commun. **302:** 324–329

33 Rao R. K., Basuroy S., Rao V. U., Karnaky K. J. and Gupta A. (2002) Tyrosine phosphorylation and dissociation of occludin-ZO-1 and E-cadherin-beta-catenin complexes from the cytoskeleton by oxidative stress. Biochem. J. **368:** 471–481

34 Kohn W.D., Kay C.M. and Hodges R.S. (1995) Protein destabilization by electrostatic repulsions in the 2-stranded alpha-helical coiled-coil leucine-zipper. Protein Sci. **4:** 237–250

35 Cohen A. R., Wood D. F., Marfatia S. M., Walther Z., Chishti A. H., Anderson J. M. et al. (1998) Human CASK/LIN-2 binds syndecan-2 and protein 4.1 and localizes to the basolateral membrane of epithelial cells. J. Cell Biol. **142:** 129–138

36 Shin H., Hsueh Y. P., Yang F. C., Kim E. and Sheng M. (2000) An intramolecular interaction between Src homology 3 domain and guanylate kinase-like domain required for channel clustering by postsynaptic density-95/SAP90. J. Neurosci. **20:** 3580–3587

37 Lue R. A., Marfatia S. M., Branton D. and Chrishti A. H. (1994) Cloning and characterization of hdlg – the human homolog of the *Drosophila* disks large tumor-suppressor binds to protein-4.1. Proc. Natl. Acad. Sci. USA **91:** 9818–9822

38 Balda M. S. and Matter K. (2000) The tight junction protein ZO-1 and an interacting transcription factor regulate ErbB-2 expression. EMBO J. **19:** 2024–2033

39 Masuko N., Makino K., Kawahara H. and Saya H. (1999) Interaction of NE-dlg/SAP102, a neuronal and endocrine tissue-specific membrane-associated guanylate kinase protein, with calmodulin and PSD-95/SAP90 – a possible regulatory role in molecular clustering at synaptic sites. J. Biol. Chem. **274:** 5782–5790